

# Phase Transformation and Band Gap Narrowing in Mechanochemically Synthesized Nitrogen-Doped TiO<sub>2</sub> for use in Dye Sensitized Solar Cell

<sup>a</sup>Samaila Buda and <sup>b</sup>Suhaidi Shafie

<sup>a</sup>Sokoto Energy Research Centre, Usmanu Danfodiyo University Sokoto

<sup>b</sup>Department of Electrical and Electronics Engineering, Faculty of Engineering, Universiti Putra Malaysia, 43400 UPM Serdang, Selangor Darul Ehsan, Malaysia

Corresponding Author's Email & Phone No.: [budasamaila@gmail.com](mailto:budasamaila@gmail.com); 08032463619

Received on: April, 2025

Revised and Accepted on: May, 2025

Published on: July, 2025

## ABSTRACT

Titanium dioxide (TiO<sub>2</sub>) is widely used as a photoanode in dye-sensitized solar cells (DSSCs), but its wide band gap (3.0–3.2 eV) restricts absorption to the ultraviolet region, limiting solar energy conversion efficiency. Nitrogen doping has been recognized as an effective strategy to extend the optical response of TiO<sub>2</sub> into the visible spectrum and improve charge separation. In this study, nitrogen-doped TiO<sub>2</sub> (N-TiO<sub>2</sub>) nanocrystals were synthesized via a mechanochemical method using high-energy ball milling of commercial TiO<sub>2</sub> (P25) in ammonium hydroxide solution. Structural and surface analyses were carried out using X-ray diffraction (XRD) and X-ray photoelectron spectroscopy (XPS). XRD results revealed that the synthesized samples consisted mainly of anatase and rutile phases, with mechanical energy promoting a partial transformation of brookite to rutile. XPS confirmed the incorporation of nitrogen into the TiO<sub>2</sub> lattice, showing distinct Ti–N and Ti–O–N bonding states. The incorporation of nitrogen decreased the band gap and expanded the spectral response of TiO<sub>2</sub> into the visible-light region, while also enhancing oxygen adsorption and reducing charge recombination. These modifications are expected to improve the photocurrent density and overall photovoltaic performance of N-TiO<sub>2</sub> based DSSCs. The findings highlight mechanochemical synthesis as a simple and effective route for producing visible-light-active N-TiO<sub>2</sub> nanomaterials for next-generation solar energy applications.

**Keywords:** Photovoltaic, nanomaterials, recombination, doping band gap

## 1.0 INTRODUCTION

Dye-sensitized solar cells (DSSCs) have emerged as one of the most promising third-generation photovoltaic technologies owing to their low fabrication cost, environmental friendliness, and relatively good performance under diffuse and indoor light conditions (O'Regan & Grätzel, 1991; Hagfeldt et al., 2010). In a typical DSSC, titanium dioxide (TiO<sub>2</sub>) is employed as the photoanode material due to its high surface area, chemical stability, low cost, and favorable electron transport properties. Nevertheless, pristine TiO<sub>2</sub> has a wide band gap of approximately 3.0–3.2 eV, which limits its absorption primarily to the ultraviolet (UV) portion of the solar spectrum. Since UV radiation accounts for less than 5% of the total solar energy, the overall power conversion efficiency of DSSCs remains restricted when using undoped TiO<sub>2</sub> (Hou et al., 2022; Ali & Sun, 2023).

To address this limitation, significant efforts have been devoted to band-gap engineering of TiO<sub>2</sub> by doping with non-metal or metal elements, sensitization with organic or inorganic dyes, and structural modification at the nanoscale. Among these, nitrogen doping has been widely studied because of its ability to narrow the band gap of TiO<sub>2</sub> by introducing localized N 2p states above the valence band, thus extending light absorption into the

visible region (Z.-Y. Han et al., 2014). Nitrogen doping not only enhances the visible-light response but also promotes charge separation, reduces electron-hole recombination, and increases photocurrent generation, which are all essential for improving DSSC performance (Kumar et al., 2021; Zhao et al., 2021).

Different synthesis techniques have been developed to incorporate nitrogen into the TiO<sub>2</sub> lattice, broadly classified into direct synthesis and post-treatment approaches. Methods such as sol-gel, solvothermal, and chemical vapor deposition fall under direct synthesis, while thermal, plasma, and hydrazine treatments are categorized as post-treatment. More recently, mechanochemical synthesis, which utilizes high-energy ball milling, has attracted growing attention due to its simplicity, cost-effectiveness, and ability to simultaneously induce nitrogen doping and phase transformations in TiO<sub>2</sub> (Tang et al., 2012). Unlike conventional thermal doping, this method provides localized high energy sufficient to break Ti–O bonds and incorporate nitrogen species into the crystal lattice at relatively low temperatures, making it a promising route for scalable DSSC electrode fabrication. (Wang et al., 2020; Chen & Zhang, 2024).

In this work, nitrogen-doped TiO<sub>2</sub> (N-TiO<sub>2</sub>) nanocrystals were synthesized using a mechanochemical approach with ammonium hydroxide as the nitrogen precursor. The structural characteristics of the samples were investigated using X-ray diffraction (XRD), while the surface chemical states were analyzed by X-ray photoelectron spectroscopy (XPS). The XRD analysis provided insights into the crystallographic phases and possible phase transformations induced by ball milling, while XPS confirmed the successful incorporation of nitrogen species into the TiO<sub>2</sub> lattice and their effect on surface electronic states. By establishing a clear correlation between nitrogen doping, phase transformation, and the resulting optoelectronic properties, this study demonstrates the potential of mechanochemically synthesized N-TiO<sub>2</sub> as an efficient photoanode material for DSSCs with enhanced visible-light absorption and photovoltaic activity.

## 2.0 MATERIALS AND METHODS

### 2.1 Synthesis methods of N-TiO<sub>2</sub>

Various methods were used in the synthesis of N-TiO<sub>2</sub>, these methods include direct synthesis and post treatment. The direct synthesis method includes; chemical vapour deposition (CVD), solvothermal process, arc discharge and mechanochemical while, Post-treatment method includes thermal treatment, plasma treatment, and N<sub>2</sub>H<sub>4</sub> treatment.

N-TiO<sub>2</sub> nanocrystals were synthesized by mechanochemical method as reported by Chao et al. (Tang et al., 2012) in which the high energy produced through ball mill was utilized to provide the needed energy to break the bonds within the TiO<sub>2</sub> crystal lattice and subsequent nitrogen doping as follows: A commercial titania powder P25 (Degussa), and ammonium hydroxide solution (NH<sub>4</sub>OH) (Kanto Chem., Japan) as a source of nitrogen were used in the synthesis. Initially, 6 g of TiO<sub>2</sub> powder was soaked in a NH<sub>4</sub>OH before putting into a reaction vessel. A planetary ball milling machine (PN100, Retsch) was used for the milling of the samples. Seven carbide tungsten balls of 15 mm diameter were introduced into an 80 ml carbide tungsten reaction vessel of the ball milling machine. The machine was operated at a rotation speed 1000 rpm for 2 hrs. The obtained wet powder was then dried at 70 °C in air. It was then sintered in a furnace at 450 °C in air for 2 hrs. Finally, a pale yellow N-TiO<sub>2</sub> powder was obtained. The resultant N-TiO<sub>2</sub> powder was grinded in a mortar to make a fined particles suitable for use in the DSSC photoanode and sample characterization.

The X-ray Photoelectron Spectroscopy (XPS) measurements were performed using a PHI II Quanterra

(ULVAC-PHI, Inc.) scanning microprobe equipped with a high efficient input lens and channel detector.

## 3.0 RESULTS AND DISCUSSION

### 3.1 Structure of the N-TiO<sub>2</sub>

In order understand the crystal nature of the synthesized N-TiO<sub>2</sub>, XRD analysis was carried out on the samples in the powder form. The result of the characterization is shown in Figure 1.

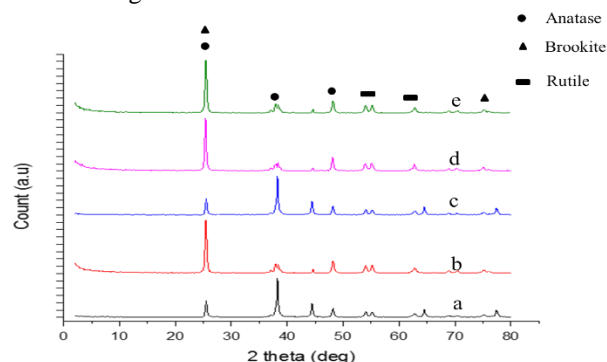


**Figure 1: The XRD pattern obtained for (a) N-TiO<sub>2</sub> 1, (b) N-TiO<sub>2</sub> 2, (c) N-TiO<sub>2</sub> 3, (d) N-TiO<sub>2</sub> 4, (e) N-TiO<sub>2</sub> 5.**

It shows that the pure TiO<sub>2</sub> is mainly of a mixture of anatase, rutile and traces of brookite phases, which is in conformity with the reference patterns JCPDS 84-1286, JCPDS 88-1175 and JCPDS No. 29-1360 respectively. The x-ray diffraction peaks at 25.5°, 38.4°, 48.0°, and 74.2° correspond to the anatase phase of TiO<sub>2</sub> and are assigned to the (101), (004), (200), and (215) crystallographic planes, respectively.

Similarly, the peaks at 54.1° and 64.0° are the diffraction peaks of the rutile phase of TiO<sub>2</sub> and are assigned to the (220) and (002) crystallographic planes, also the peak at 67.3° is a diffraction peak of brookite, while the main (101) diffraction peak of anatase at 25.5° overlaps with the (120) and (111) peaks of brookite at 25.34° and 25.69°, respectively, therefore, a pure anatase sample could be a mixture of both the anatase and brookite (Paola et al., 2013). There is no visible nitrogen diffraction peaks in the XRD diffraction patterns of the N-TiO<sub>2</sub>, indicating that the doping element is dispersed in TiO<sub>2</sub> structure with a high degree (Z.-Y. Han et al., 2014).

The mechanical energy treatment of TiO<sub>2</sub> through planetary ball milling has resulted in the gradual transformation of the trace amount of brookite form of P25 into rutile form as seen by the disappearance of the diffraction peak at 67.3 attributed to the brookite structure.

Generally, the thermal energy needed for this transformation is within the temperature range between 700 °C and 800 °C. These results suggested that high mechanical energy results in the phase transformation of brookite to rutile form.

### 3.2 X-ray Photoelectron Spectroscopy (XPS)

XPS is a surface (2 to 10 atomic layer depth) analysis technique that allows determination of the chemical composition as well as chemical environment of atoms of a thin layer or the top surface of a specimen through bombardment of the sample with x-ray in a high vacuum chamber which leads to ejection of secondary electron from the specimen. The energy of the ejected electrons ( $E_k$ ) is related to the photon energy and electron binding energy ( $E_b$ ) through the relationship.

$$E_k = h\nu - E_b \quad (3.10)$$

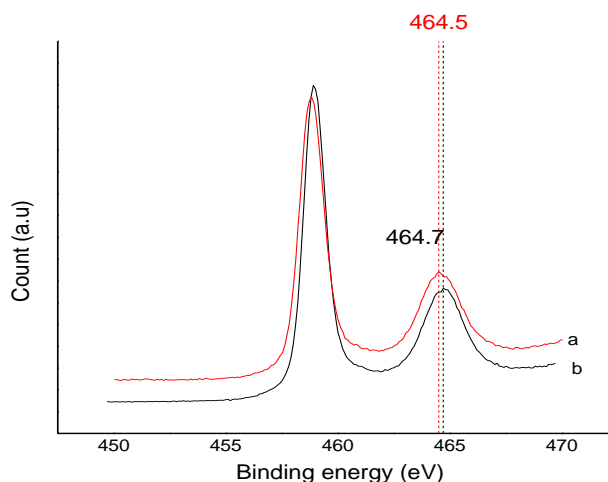


**Figure 2. XPS narrow scan for N-TiO<sub>2</sub> (a) before doping, (b) after doping.**

The XPS spectra of the TiO<sub>2</sub>, and N-TiO<sub>2</sub> provided an insight of their chemical structures and are shown in Figure 2. Figure 2a shows the Ti 2p spectra for the pure TiO<sub>2</sub> sample, in which two prominent peaks are observed at 458.8 and 464.4 eV corresponding to the binding energies of the Ti 2p<sup>3/2</sup> and Ti 2p<sup>1/2</sup> core levels due to the presence of the Ti (IV) (Kang et al., 2010). Also, Figure 2b shows the narrow scans for the Ti 2p peaks of N-TiO<sub>2</sub>, the binding energy of Ti 2p becomes higher after ammonium impregnation. The increase of Ti 2p binding energy indicates that the electro positivity of titanium ions on the surface increases. The changes of the chemical state on the surface improve the oxygen adsorption capacity of the catalyst surface, and reduce the combination rate of e<sup>-</sup>-h<sup>+</sup> leading to the photovoltaic activity of the photoelectrode being improved (Z.-Y. Han et al., 2014)

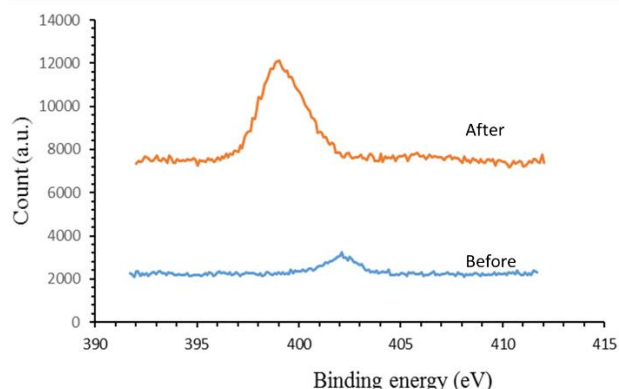


**Figure 3. XPS spectra showing the presence of nitrogen in the N-TiO<sub>2</sub> structure.**

Figure 3 shows the narrow scans for the nitrogen peaks which supported the existence of nitrogen in the doped TiO<sub>2</sub> powder. The nitrogen peak at 398.9 eV is a substitution of Ti with N into TiO<sub>2</sub> lattice sites caused by high mechanical energy induced on TiO<sub>2</sub> during the milling process. While the peak at 402.0 eV is attributed to N in the chemical adsorption of N into the TiO<sub>2</sub>.

The N atoms chemically bonding with the N 1s XPS peak at 398.9 eV and 402.0 eV obtained from N-TiO<sub>2</sub> are assigned to Ti-N bonding due to the substitutional N dopants while Ti-O-N is due to the interstitial N, respectively. The tail in the N 1s peak at 398.9 eV was derived from absorbed oxygen forming the Ti-N-O band.

N doping decreases the forbidden band width of TiO<sub>2</sub>, and expands the spectral response of the material to a visible light region, so it improves the photovoltaic activity of the semiconductor. In addition, N doping makes oxygen defect appears on the TiO<sub>2</sub> surface which is beneficial for the reduction of charge recombination within the material (Z.-Y. Han et al., 2014). The binding energy of the N1s at 400.26 eV of the N-TiO<sub>2</sub> suggests that nitrogen atoms replace some of the Ti in the TiO<sub>2</sub> surface thereby forming N-OTi, which in effect causes some changes of the electron density around the oxygen atoms. Therefore, N-doped is the replacement doping rather than the adsorption.

### 4.0 CONCLUSION

Mechanical ball milling of TiO<sub>2</sub> in ammonium solution can produce enough energy required for doping of nitrogen in the TiO<sub>2</sub> crystal structure. This claim is supported by the XPS spectra of N-TiO<sub>2</sub>. Phase transformation of anatase to rutile can also be achieved with increasing mechanical energy milling. However, prolonged milling of titania powder in ammonium solution could result in having excess nitrogen in the titania



structure which negatively affect power conversion efficiency of N-TiO<sub>2</sub> based dye sensitized solar cell. Incorporation of nitrogen in the TiO<sub>2</sub> can causes visible light absorption of the TiO<sub>2</sub> which improves the photocurrent density of the N-TiO<sub>2</sub> based DSSC,

## REFERENCE

- Ali, F., & Sun, L. (2023). Advances in N-doped TiO<sub>2</sub> nanostructures for photovoltaic applications. *Journal of Photochemistry & Photobiology A: Chemistry*, 439, 114525. <https://doi.org/10.1016/j.jphotochem.2022.114525>
- Chen, Y., & Zhang, S. (2024). Recent developments in heteroatom-doped TiO<sub>2</sub> for solar energy devices. *Advanced Materials Interfaces*, 11(3), 2301456. <https://doi.org/10.1002/admi.202301456>
- Hagfeldt, A., Boschloo, G., Sun, L., Kloo, L., & Pettersson, H. (2010). Dye-sensitized solar cells. *Chemical Reviews*, 110(11), 6595–6663. <https://doi.org/10.1021/cr900356p>
- Hou, Y., Sun, L., & Kloo, L. (2022). Recent progress in dye-sensitized solar cells with modified TiO<sub>2</sub> photoanodes. *Solar Energy Materials and Solar Cells*, 240, 111707. <https://doi.org/10.1016/j.solmat.2022.111707>
- Kumar, R., Singh, P., & Verma, N. (2021). Mechanochemical synthesis of doped TiO<sub>2</sub> for

- enhanced visible light activity. *Materials Chemistry and Physics*, 270, 124853. <https://doi.org/10.1016/j.matchemphys.2021.124853>
- O'Regan, B., & Grätzel, M. (1991). A low-cost, high-efficiency solar cell based on dye-sensitized colloidal TiO<sub>2</sub> films. *Nature*, 353(6346), 737–740. <https://doi.org/10.1038/353737a0>
- Tang, Y., Zhang, Y., Wang, Z., & Chao, C. (2012). Mechanochemical synthesis and photocatalytic activity of nitrogen-doped TiO<sub>2</sub>. *Materials Letters*, 68, 248–251. <https://doi.org/10.1016/j.matlet.2011.10.089>
- Wang, T., Li, X., & Zhang, F. (2020). Band gap engineering in TiO<sub>2</sub>-based DSSCs: A review. *Renewable and Sustainable Energy Reviews*, 132, 110080. <https://doi.org/10.1016/j.rser.2020.110080>
- Zhao, Y., Chen, J., & Wang, H. (2021). Electronic structure tuning of nitrogen-doped TiO<sub>2</sub> for solar energy conversion. *Applied Surface Science*, 566, 150664. <https://doi.org/10.1016/j.apsusc.2021.150664>
- Z.-Y. Han, Y., Wang, F., & Zhang, W. (2014). Nitrogen-doped TiO<sub>2</sub> photocatalysts for visible light applications: A review. *Catalysis Today*, 225, 30–40. <https://doi.org/10.1016/j.cattod.2013.10.021>